Journal of Power Sources 248 (2014) 1133–1140

Contents lists available at ScienceDirect

Journal of Power Sources

journal homepage: www.elsevier.com/locate/jpowsour

Seeking effective dyes for a mediated glucose–air alkaline battery/fuel cell

Ross Eustis [a], Tsz Ming Tsang [b], Brigham Yang [b], Daniel Scott [b], Bor Yann Liaw [a,*]

[a] Hawaii Natural Energy Institute, SOEST, University of Hawaii at Manoa, 1680 East West Road, POST 109, Honolulu, HI 96822, USA
[b] Department of Biochemistry, Brigham Young University-Hawaii, 55-220 Kulanui Street, Laie, HI 96762, USA

HIGHLIGHTS

- Important aspects in solubility and mobility for 45 redox dyes in alkaline solutions are discussed.
- Polarization effects related to mass transport limitation on indigo and its sulfonate derivatives are explained.
- Optimization strategy for power generation using a matrix of dye selection is presented.
- Co-solvent effect on dye solubility and mobility is studied.
- Loss from mass transport limitation versus other kinetic factors was analyzed to guide future work.

ARTICLE INFO

Article history:
Received 9 August 2013
Received in revised form
1 October 2013
Accepted 7 October 2013
Available online 15 October 2013

Keywords:
Glucose–air alkaline battery/fuel cell
Redox dye mediator
Partial oxidation of glucose
Indigo carmine
Peak power density
Maximum power point

ABSTRACT

A significant level of power generation from an abiotic, air breathing, mediated reducing sugar–air alkaline battery/fuel cell has been achieved in our laboratories at room temperature without complicated catalysis or membrane separation in the reaction chamber. Our prior studies suggested that mass transport limitation by the mediator is a limiting factor in power generation. New and effective mediators were sought here to improve charge transfer and power density. Forty-five redox dyes were studied to identify if any can facilitate mass transport in alkaline electrolyte solution; namely, by increasing the solubility and mobility of the dye, and the valence charge carried per molecule. Indigo dyes were studied more closely to understand the complexity involved in mass transport. The viability of water-miscible co-solvents was also explored to understand their effect on solubility and mass transport of the dyes. Using a 2.0 mL solution, 20% methanol by volume, with 100 mM indigo carmine, 1.0 M glucose and 2.5 M sodium hydroxide, the glucose–air alkaline battery/fuel cell attained 8 mA cm^{-2} at short-circuit and 800 μW cm^{-2} at the maximum power point. This work shall aid future optimization of mediated charge transfer mechanism in batteries or fuel cells.

1. Introduction

The demand for sustainable alternative energy is growing rapidly worldwide [1]. Renewable resources such as solar, wind, or biofuels are attractive to many to achieve carbon neutral energy conversion. Electrochemical energy conversion is one of the most efficient methods to convert chemical energy into electrical. Primary batteries or fuel cells promise high theoretical efficiency [2,3]. Advanced primary battery systems using metal–air (e.g. lithium–air or zinc–air) reactions continue to attract attention by the energy storage community, even though commercialization is still impeded by technical barriers that inhibit the redox reaction [4–8]. Presently, hydrogen and methanol are each advocated as the future in clean energy, however both cost too much for large-scale applications. Novel fuel cells that harness energy from carbon-rich fuels, such as glucose, provide an affordable alternative. Such biotic fuel cells already show promise at lower power densities [9].

Higher power densities are possible by optimizing the catalysts that function on the cathode and anode. Improved oxygen reduction on the cathode would decrease polarization interference in the existing fuel cell [10]. Non-noble metal catalysts are of particular interest and are currently being explored [11]. Catalysis of carbon-rich fuels on the anode can also be improved. Platinum (Pt) has been the most used catalyst so far [12]. However, Pt is both costly and scarce. Complete oxidization of glucose down to CO_2 is a

* Corresponding author. Tel.: +1 808 956 2339; fax: +1 808 956 2336.
E-mail addresses: bliaw@hawaii.edu, boryann.liaw@gmail.com (B.Y. Liaw).

0378-7753/$ – see front matter © 2013 Elsevier B.V. All rights reserved.
http://dx.doi.org/10.1016/j.jpowsour.2013.10.022

desirable process difficult to realize in a conventional fuel cell or bio-fuel cell. A new method of harnessing electrical energy from carbohydrates (e.g. glucose) is highly desired [13]. Past experimentation has been seeking for alternative pathways for catalyzed glucose oxidation [9,14–24]. Enzymatic catalysts have been pursued to mimic glycolysis [14–16]. Microbial fuel cells could simplify the energy harvesting process [17,18]. It is known that mediated charge transfer can achieve effective catalysis [16,19]. With mediated charge transfer, a reducing sugar–air alkaline battery (SAAB) has been demonstrated in our laboratory, which operates at ambient pressure and temperature, producing a peak power density (PPD) on the order of a few mW cm^{-2} [20,21]. Partial oxidation of monosaccharides occurs naturally in strong alkaline solution, requiring no catalyst to yield an ene-diol intermediate. What

Table 1
A comparison of 45 redox dyes to function as electron mediators: molar mass, relative solubility in the nominal solution (see key), current density at short-circuit, cell open circuit voltage, formal reduction potential and diffusivity are shown for each dye in the alphabetical order. Nominal test solutions contain 50 mM dye, 1.0 M glucose, and 2.5 M NaOH. Citations for the formal reduction potential are also included in the footnotes.

Dye	Molar mass (g mol^{-1})	Relative solubility	Current density (mA cm^{-2})	Cell voltage (mV)	E° (mV vs SCE)	D (m^2 s^{-1})	Refs[a]
ABTS	548.7	3	0.100 ± 0.007	403 ± 27	−399	59.14	1
Alizarin red S	342.3	1	0.30 ± 0.02	538 ± 36	−1079	53.50	2
Alizarin yellow GG	309.2	2	0.90 ± 0.06	90 ± 6	−220	60.25	3
Benzenesulfonic acid, Na salt	180.2	3	0.0	491 ± 33	N/A	N/A	–
Brilliant blue R	826.0	2	0.100 ± 0.007	520 ± 35	−236	9.37	4
Brilliant green	482.6	1	0.0	468 ± 31	−485	5.56	3
Brilliant yellow	624.6	3	0.100 ± 0.007	540 ± 36	−381	3.86	3
Bromocresol purple	540.2	2	0.70 ± 0.05	559 ± 38	−117	7.51	3
Cresyl violet	321.3	2	0.70 ± 0.05	583 ± 39	−680.3	5.08	5
DTNB	396.4	3	1.5 ± 0.1	496 ± 33	−441	12.83	3
Erythrosine	835.9	2	0.100 ± 0.007	374 ± 25	−437	29.51	3
Fast green	765.9	2	0.5 ± 0.03	588 ± 39	−183	10.24	3
Hydroquinone	110.1	3	1.5 ± 0.1	501 ± 34	−274	30.01	6
Indigo carmine (IC)	466.3	2	4.00 ± 0.03	510 ± 34	−687	10.09	6
Indigo tetrasulfonate (ItetS)	734.88	3	3.80 ± 0.03	441 ± 30	−402	N/A	7
Indigo trisulfonate (ItriS)	616.7	3	3.20 ± 0.02	479 ± 32	−435	N/A	7
Indocyanine green	775.0	2	0.0	360 ± 24	N/A	N/A	–
Janus green	511.1	0	0.100 ± 0.007	459 ± 31	−469	20.96	8
Light green SF yellowish	749.9	2	0.70 ± 0.05	600 ± 40	−569	0.53	3
Malachite green oxalate	927.0	0	0.30 ± 0.02	578 ± 39	−506.427	0.95	3
[b]Methoxatin disodium salt (PQQ)	374.2	3	2.0 ± 0.1	450 ± 30	−323	N/A	9
Methyl blue	799.8	2	1.00 ± 0.07	561 ± 38	−576	33.61	3
Methyl orange	327.3	1	0.0	545 ± 37	−332.5	5.66	3
Methyl viologen (MV)	257.2	3	4.20 ± 0.03	626 ± 42	−684	36.72	8
Methylene blue	319.9	1	0.3	470 ± 32	−235	39.68	7
Methylene green	433.0	1	1.5 ± 0.1	504 ± 34	−649	N/A	3
Neutral red	288.8	1	0.5 ± 0.03	207 ± 14	−198	30.04	8
Nicotinamide	122.1	2	0.0	468 ± 31	−559	19.17	3
Nile blue A	353.9	0	0.40 ± 0.03	499 ± 33	N/A	N/A	–
Phenolphthalein	318.3	3	0.30 ± 0.02	473 ± 32	−492	28.77	3
Potassium ferricyanide	329.3	3	0.100 ± 0.007	518 ± 35	−1044.6	53.63	3
Pyromellitic dianhydride	218.1	3	0.30 ± 0.02	509 ± 34	−142	6.62	3
Quinalizarin	272.2	3	1.00 ± 0.07	523 ± 35	73.0	7.71	6
Reactive red 120	1470.0	3	0.5 ± 0.03	485 ± 33	−196	5.90	4
Sodium diphenylamine sulfonate	271.3	2	0.100 ± 0.007	376 ± 25	−336	N/A	10
Sudan black	456.5	0	0.0	489 ± 33	−634	13.46	3
Indigo	262.3	0	0.20 ± 0.01	561 ± 38	N/A	4.14	–
Tartrazine	534.3	3	0.100 ± 0.007	539 ± 36	−485	32.14	3
Terephthalic acid	166.1	3	0.100 ± 0.007	530 ± 36	−565	0.84	3
Thiophene-3,4-dicarboxylic acid	172.2	3	0.100 ± 0.007	434 ± 29	N/A	N/A	–
Thymol blue	466.6	2	0.5 ± 0.03	510 ± 34	−459	1.89	3
Thymolphthalein	430.6	2	0.100 ± 0.007	432 ± 29	−252.7	30.07	11
Trypan Blue	872.9	3	1.00 ± 0.07	620 ± 42	−429	7.17	3
Vanadium oxide (V)	181.88	3	0.70 ± 0.05	421 ± 28	−760	N/A	12
2,6-Dichlorophenolindophenol	268.1	2	1.5 ± 0.1	258 ± 17	−412.8	N/A	13

[1] Ref. [30].
[2] Ref. [31].
[3] This work.
[4] Ref. [32].
[5] Ref. [33].
[6] Ref. [34].
[7] Ref. [35].
[8] Ref. [36].
[9] Ref. [37].
[10] Ref. [38].
[11] Ref. [39].
[12] Ref. [40].
[13] Ref. [41].
Solubility key: 0 = not soluble; 1 = slightly soluble; 2 = mostly soluble; 3 = completely soluble.
[a] Notes: Citations for formal potential (E°).
[b] Note: The conc. of PQQ used was 2.5 mM.

enables high PPD is the electron mediator that shuttles two electrons per glucose to the carbon anode surface, stabilizing the enediol to gluconolactone or gluconic acid. The redox potential of the mediator is sufficiently negative against oxygen reduction in a strong alkaline solution. Thus, oxidation of the reduced mediator only occurs at the anode. At the cathode, oxygen is reduced to hydroxide ions via the catalysis of Pt or much less costly MnO_2 [25]. The SAAB utilizes partial oxidation of glucose to gluconic acid with a coulombic efficiency approaching 100%, reaching energy and power density comparable to most metal–air counterparts to date. It can rival ethanol combustion, if considering the efficiency of sugar fermentation and cost of alcohol purification [26].

The SAAB is an attractive alternative energy source, yet its PPD is limited by mass transport of the mediator, as our prior work suggests [20,21]. The mass transport limitation prompts us to conduct this study aiming to seek better conduction of the mediator for higher power density in performance. Here we investigated 45 redox dyes for their potential in enhancing mass transport in the SAAB. Several aspects that might be useful in improving dyes' mass transport behavior in the alkaline solution include: (1) dye's solubility, (2) the valence charge carried by each dye, (3) the size of the dye (i.e. its molecular weight (MW) in general). To address aspect (1), co-solvents (e.g. methanol, ethanol, acetone, dimethyl sulfoxide (DMSO), glycerol, acetonitrile, 2-propanol, and pyridine) were explored to seek improvements in dye's solubility. For dye selection, the following aspects were used in a preliminary screening: (1) the open circuit voltage (OCV) of the SAAB, which gives the formal redox potential of the dye against the oxygen reduction; (2) polarization in the SAAB; (3) the short-circuit current density (I_{SC}), which describes the mass transport kinetics; (4) MW, as an indicator of the steric constraint of the dye; and (5) a visual assessment of relative solubility of the dye in the SAAB solution. Through this preliminary study, we hope to develop an optimized strategy for an SAAB with higher power output and a useful guideline for future improvements.

2. Experimental

ACS reagent D-(+)-glucose and most redox dyes were purchased from Sigma–Aldrich. Dyes unavailable through Sigma–Aldrich were purchased from others such as Frontier Scientific, MCB Reagents, Harleco, EM Scientific, National Biological Stains & Reagents Department, Matheson Coleman & Bell, and Eastman Kodak. Reagents such as NaOH, KOH, HCl, DMSO, methanol, ethanol, acetone and additional dyes were purchased from Fischer Scientific. A full list of the 45 redox dyes is provided in Table 1.

Fig. 1 shows the schematic of the test cell configuration. A piece of 3.18 mm thick carbon felt (Alfa Aesar) was used as the current collector at the negative electrode (anode). The positive electrode (cathode) has an air-breathing catalyst composed of a silver-plated nickel screen with 0.6 mg cm^{-2} TM loading of 10% Pt on Vulcan XC-72 with microporous fluorocarbon backing (BASF). A plastic cap with opening to air held the cathode, allowing the catalyst in contact with oxygen while sealing the reaction chamber to minimize evaporation. Pt wire was used to connect electrodes in the test cell to minimize possible background current leakage due to corrosion or parasitic side reactions. Although Pt could act as a catalyst for glucose oxidation, experiments without a mediator produced only a negligible amount of current, easing concerns of any side effect from the Pt leads. All electrochemical measurements were conducted with a Bio-Logic 16-channel VMP3 or a 2-channel VSP potentiostat.

In the preliminary screening of dyes, the nominal test solution for each experiment was 2.0 mL of 1.0 M glucose, 2.5 M NaOH and 50 mM redox dye. A concentration of 50 mM exceeds the solubility

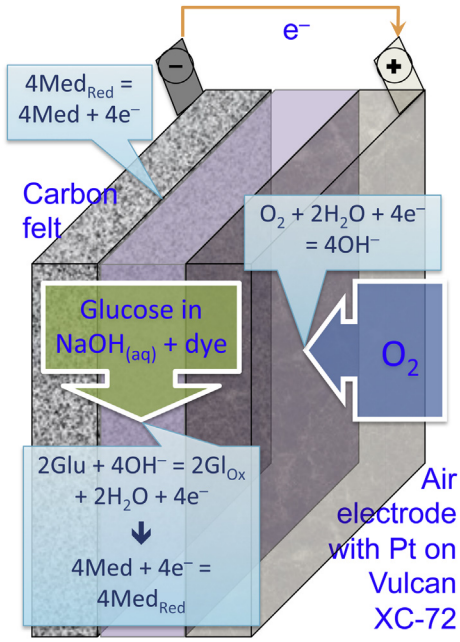

Fig. 1. Schematic of the cell configuration.

of most redox dyes in the study. This concentration was used in the screening to estimate the relative solubility of each dye on a scale of 0–3; "zero" meaning insoluble and "3" completely soluble, as denoted in Table 1. Any un-dissolved dye was not filtered from solution. Instead, it was allowed to settle before the saturated solution above the settlement was extracted for experimentation. Test solutions were not heated to dissolve the dye.

Indigo and its sulfonate derivatives: indigo carmine (IC), indigo trisulfonate (ItriS), and indigo tetrasulfonate (ItetS), were used to further investigate the impact of molecular structure on mass transport properties. Polarization and I_{SC} of IC were studied as a function of (1) the number of sulfonate groups, (2) concentration of IC in 20% vol. DMSO, (3) polar co-solvents, and (4) methanol concentration in % vol. This family of indigo dyes provides a case study on the effect of molecular structure with various numbers of sulfonate groups on mass transport. Co-solvents used, all at 20% vol., are: methanol, ethanol, acetone, DMSO, glycerol, acetonitrile, 2-propanol, and pyridine. For a comparison of polar co-solvents, a nominal 75 mM IC was used to explore the solubilization effect. As methanol performed the best among all, the optimal % vol. of methanol was determined and characterized for its performance in SAAB.

3. Results

Table 1 summarizes the MW, relative solubility, I_{SC} and cell OCV of the 45 redox dyes, listed by relative solubility, MW, and cell OCV to assess their potential as mediators in the SAAB. Methyl viologen (MV) has the highest solubility, OCV, and I_{SC}, and low MW, remaining as the top contender so far. The indigo sulfonate derivatives (IC, ItriS and ItetS) are competitive to MV in term of I_{SC}, but each suffers from a lower OCV and solubility, and a higher MW. The indigo dyes remain attractive as alternatives to MV due to lower toxicity. The properties among indigo and its sulfonate derivatives are also exhibited in Table 1. As the number of sulfonate group increases in indigo, MW and solubility increase, but OCV poses a gradual decrease. IC has the highest I_{SC}, although ItriS and ItetS are comparable. Indigo is insoluble in the nominal test solution; thus,

its conductivity and I_{SC} are noticeably compromised. Also included in Table 1 are formal reduction potential and diffusivity of the dyes in the test solution. The formal reduction potentials are derived from either the cyclic voltammetric (CV) experiments (not reported herein) or the data reported in the literature, as indicated in the last column as citations in the footnotes of the table. Since the CV experiments were not performed at the standard state condition, the formal reduction potential is reported for the test conditions against a standard calomel electrode (SCE). The limited solubility of the dyes also prevented us from deriving the activity coefficient of the dyes as a function of concentration to estimate the standard reduction potential. The diffusivity of the dyes was derived from the respective I_{SC}, as a result of the approximation of the Fick's law at the test condition. One should be mindful that the I_{SC} is the limiting current under the partial oxidation of glucose via the shuttling process of the dye. The diffusivity as derived from the limiting current might be different from those measured under a chemical potential (as created by a concentration gradient) or a simple electric field (as imposed by voltammetry).

The polarization curves of IC, ItriS and ItetS are shown in Fig. 2. As the number of the sulfonate groups increases, polarization resistance increases while I_{SC} decreases slightly. Fig. 3(a) gives the polarization curves of 50, 75 and 100 mM IC with co-solvent DMSO at 20% vol. As the IC concentration increases in the solution, the polarization resistance decreases, and I_{SC} increases incrementally in a linear fashion, as shown in Fig. 3(b).

Fig. 4 displays polarization curves of 75 mM IC in the presence of four co-solvents (i.e. methanol, ethanol, acetone, and DMSO), each at 20% vol. Acetonitrile, 2-propanol, pyridine and glycerol were omitted as they performed worse than the four. Methanol is the best among the four, minimizing the polarization the most and achieving the highest I_{SC}. Ethanol produces a comparable effect on polarization but a lower I_{SC}. In Fig. 5, the effect of methanol % vol. on I_{SC} in a 50 mM IC solution is shown. At compositions less than 15% vol., I_{SC} increased linearly with methanol content, suggesting that IC solubility had indeed increased with the addition of methanol as a co-solvent. At compositions greater than 15% vol., I_{SC} began to decrease and reached a stable 5.5 mA cm^{-2} at 25% vol. methanol or higher. The highest I_{SC} of 7.2 mA cm^{-2} occurs at 15% vol. methanol in solution.

Fig. 6 compares the polarization curves and power density profiles for two SAABs: (1) a 50 mM IC test cell without co-solvent, and (2) a 100 mM IC test cell with 15% vol. methanol. The I_{SC} of test cell #2 is roughly double that of test cell #1, yet both achieve a similar PPD. The maximum power point (MPP), which labels the current density–PPD correspondence, is however about the same in both cases. The power density profile of test cell #1 has a "crippled" deviation, in contrast to that of test cell #2, as the curve approaches the MPP before the short-circuit.

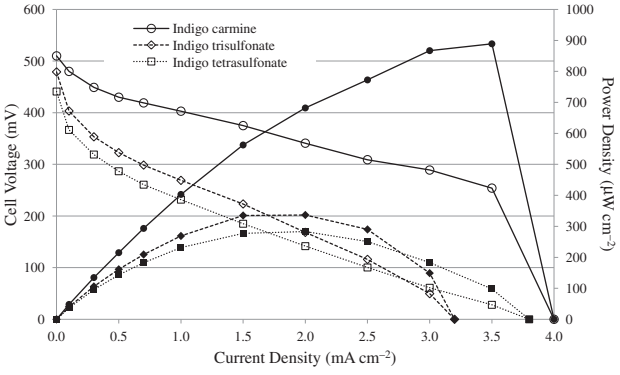

Fig. 2. Polarization curves of the sugar–air alkaline battery (SAAB) with IC, ItriS, and ItetS, each at 50 mM in nominal solutions.

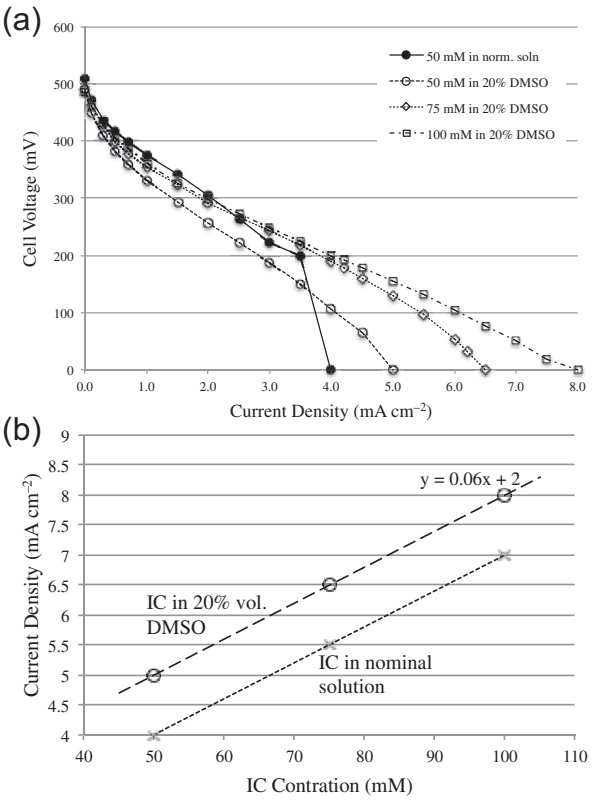

Fig. 3. (a) Polarization curves of the SAAB with 50, 75, and 100 mM IC in 20% vol. DMSO. (b) I_{SC} from the polarization curves in (a) follows a linear relationship with IC content in an electrolyte solution with 20% vol. DMSO (dashed line). A similar trend line (dotted line) projected for the nominal solution without DMSO is also shown to illustrate an "equivalent" concentration concept that can be used to quantify the enhancement in solubility by the co-solvents.

4. Discussion

4.1. Useful considerations for dye selection

The operation of SAAB demands highly soluble, mobile mediators to facilitate high energy-conversion efficiency and PPD. The mediators should exhibit a highly negative redox potential, but should not surpass (become more negative than) the oxidation potential of the carbohydrates. If so, the mediator would not be able to accept charge, thus shutting down the electron transfer process. The mediator must also interact with the oxidant intermediate effectively to aid charge transfer. The mechanism of such an interaction is not yet fully characterized, but favorable steric interaction between the donor and acceptor functional groups must be crucial for effective charge transfer. As mass transport is most critical in this work, we focused on improving dye solubility and mobility. Although solubility can be considered from the perspective of functional groups in a redox dye in the presence of solvent, it is not trivial to derive quantitative correlations among the functional groups, redox potential, and rate of electron transfer in a predictive manner. In this work, we thus rely on some empirical derivations from the variations in PPD and I_{SC} with dyes of different functional groups to provide insightful information on the role the functional groups plays in charge transfer kinetics.

The redox reaction at the anode should follow a multi-step mechanism (Ref. [27] offers some relevant discussions): (1)

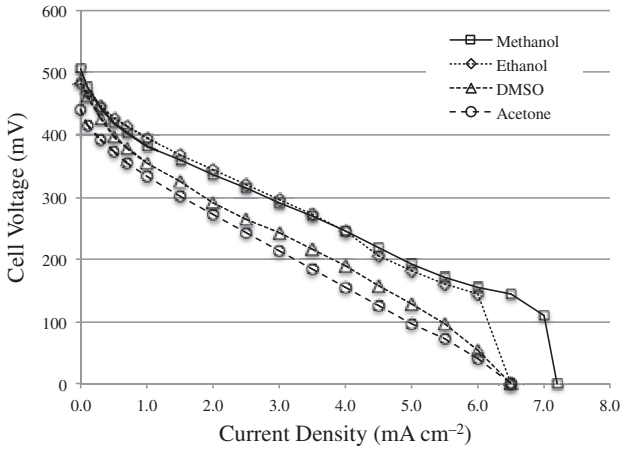

Fig. 4. Polarization curves of the SAAB with 75 mM IC and four polar co-solvents: methanol, ethanol, acetone, and DMSO (each at 20% vol.).

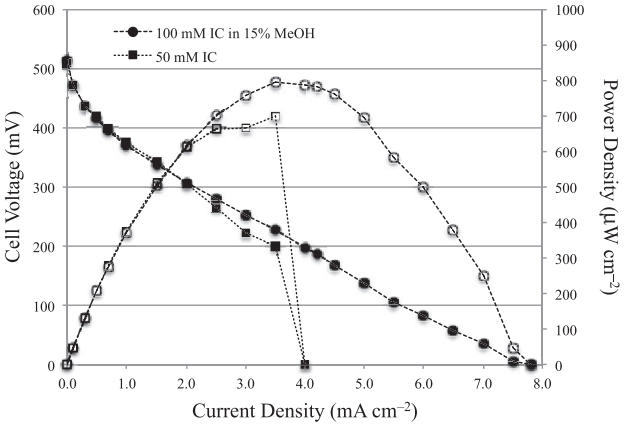

Fig. 6. Polarization curves and power density profiles of a 50 mM IC nominal cell and a cell of 100 mM IC with 15% vol. methanol.

monosaccharide oxidation to form the ene-diol intermediate, (2) dye reduction by charge transfer from the ene-diol intermediate, (3) diffusion and migration of the reduced dye to the anode current collector, and (4) charge transfer from the dye to the anode current collector, reverting the dye back to its unreduced, charged state, (5) dye diffusion back into solution. The electron shuttling by the dyes should continue via steps (2)–(5) until the ene-diol intermediate concentration reaches below a threshold to retard the shuttling process. To select promising dyes for maximum power output, the following aspects were considered:

- Step (1) is likely independent of the dye or its concentration, as suggested by our prior work [20,21]. This realization is very vital in formulating the optimization strategy for the energy conversion process. This step is considered a result of chemical equilibrium among various isomers of monosaccharide and partial oxidation products (i.e. gluconolactone and gluconic acid). This is also an arguable result that the mediator is not a catalyst in this process. Instead, the mediators perturb the complex equilibrium via electron shuttling that changes the balance in the concentration of the species in the solution where the source of electrons were created from the glucose (isomer) partial oxidation, as described by the Le Chatelier's principle.
- Steps (2) and (4) should depend on the kinetics of charge transfer and redox reversibility of a dye.
- As suggested from our prior work [20,21], the rate-limiting step for power production seems to hinge on the mass transport of the dye. Thus, the analysis of the rate capability of the dyes is most crucial. To enhance mass transport of the dye, we considered the following aspects:
  a) Increase dye solubility in the solution, while maintaining a highly negative redox potential.
  b) Increase dyes mobility.
  c) Increase the valence charge a dye shuttles.

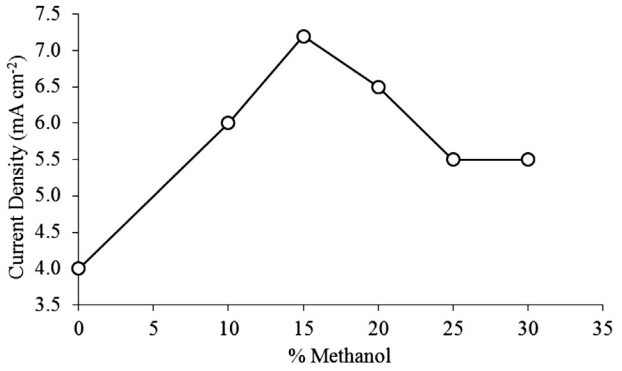

Fig. 5. Effect of methanol content on the I_{SC} in an SAAB with 75 mM IC.

To assess aspect (a), the dye solubility in the alkaline solution was indexed in Table 1. Among the 19 dyes completely soluble at 50 mM (as visually inspected and labeled by a solubility rating of 3), MV (626 mV) and Trypan Blue (620 mV) give the highest OCV in SAAB. A subsidiary group in Table 1 comprises the remaining 17 soluble dyes whose OCVs range from 540 to 400 mV. After MV and Trypan Blue, the difference in OCV between any two adjacent dyes is quite subtle.

MW affects a species' mobility and diffusion in solution. The low MW (257.2 g mol^{-1}) of MV together with its high solubility attains a high $I_{SC} = 4.2$ mA cm^{-2}. In contrast, Trypan Blue, with solubility and OCV comparable to MV, has a much higher MW (3.4 fold) and achieves an $I_{SC} = 1.0$ mA cm^{-2}. ItetS (3.8 mA cm^{-2}; 734.88 g mol^{-1}), ItriS (3.2 mA cm^{-2}; 616.7 g mol^{-1}), and PQQ (2.0 mA cm^{-2}; 374.2 g mol^{-1}) are also attractive dyes despite lower OCVs. The remaining soluble dyes fall short of attaining an I_{SC} much greater than 1 mA cm^{-2}. Among the remaining less-soluble dyes in Table 1, IC shows interesting potential. Even though IC is not completely soluble at 50 mM (solubility rating of 2) and has an MW (466.3 g mol^{-1}) roughly twice that of MV, it reached an $I_{SC} = 4.0$ mA cm^{-2}.

Similarities in molecular structure between MV and IC suggest characteristics important to a mediator in the SAAB operation. The relatively small size of each dye would correspond to fast diffusion. MV and IC each contains an electronegative, heterocyclic amine group [28], which could be crucial in stabilizing the reduced, charge-carrying dye in the transport mechanism. MV and IC also have high degrees of steric symmetry. According to kinetic theory, a higher degree of symmetry would improve the probability of successful charge transfer between the ene-diol and dye as well as the anode and reduced dye. The importance of structure, symmetry and size should be considered in future investigation and selection of redox dyes as mediators. IC was further investigated in this study, due to its lower toxicity and its sulfonate group function.

4.2. Effect of sulfonate groups on the kinetic behavior of indigo dyes

The family of indigo dyes with sulfonate derivatives (i.e. IC, ItriS, and ItetS) provides us an interesting opportunity to study the

function of sulfonate groups in the electron shuttling process. Fig. 7 exhibits the structural formulas of indigo, ItriS, and ItetS. Addition of sulfonate groups to indigo dye substantially increases solubility, as seen in Table 1 [29]. However, the presence of sulfonate groups also results in a decrease in cell OCV. Although adding two sulfonate groups to indigo (i.e. IC) reduces cell OCV from 561 mV to 510 mV, PPD actually increases by a factor of 20 (Table 1). The I_{SC} of indigo is extremely low as indigo is insoluble in solution. IC appears to achieve the optimal functionality of sulfonate groups in the dye in energy conversion process, as shown in Fig. 2. Although adding sulfonate groups improves dye's solubility, it does not lead to higher I_{SC} but continues a decline in cell OCV, as exhibited by ItriS (479 mV) and ItetS (441 mV). On one hand, the steric drag caused by the bulk and mass of a sulfonate group could hinder diffusion. On the other, the additional charge of a sulfonate group could stabilize the reduced dye in charge transport and migration to the anode. At the same time, additional charge could affect solvation [29], increasing interactions with polar solvent molecules, marginalizing drift. It is evident that adding sulfonate groups into the dye molecular structure improves dye solubility, as expected; yet, the complicated interplay of physicochemical and electrochemical interactions on the charge transport mechanism of the dye collectively vary I_{SC} and polarization as the number of sulfonate groups in the dye increases.

At a concentration of 50 mM, IC exhibited the best conductivity among the three sulfonate indigo dyes, as evidenced by the least polarization (between 0.5 and 3.5 mA cm^{-2}) in the curves shown in Fig. 2. However, IC reaches the mass transport limitation (between 3.5 and 4.0 mA cm^{-2}) to yield an $I_{SC} = 4.0$ mA cm^{-2}. As sulfonate group increases from IC to ItetS, polarization resistance also increases due to the declining ionic conductivity, as suggested by the slope of the polarization curves. ItetS has a lower ionic conductivity than ItriS, as the higher polarization in the curve indicates. Interestingly, ItriS exhibits a polarization curve with an early influence by mass transport starting at 1.5 mA cm^{-2}, as shown by the deviation from the linear ohmic regime, which gradually descends to an $I_{SC} = 3.2$ mA cm^{-2}. ItetS, in contrast, exhibits little influence from mass transport limitation, as its ohmic polarization regime extends to almost 3.5 mA cm^{-2} before reaching the $I_{SC} = 3.8$ mA cm^{-2}, close to that of IC. As a brief summary, it is fair to say that the addition of the sulfonate groups to the indigo dyes increases their solubility in the alkaline solution, and the sulfonate group–solvent interactions may have facilitated the charge transfer in the solution, as in the case of IC. Beyond that, the addition of sulfonate groups also creates a complicated effect on the mobility of the dye and solubility, as implied from the increase in polarization resistance and the extension of the linear ohmic polarization regime in the polarization curve in ItetS, but not in ItriS. The complexity could come from the solvation and the ion–polar solvent interaction. Sulfonate groups also increased the polarization in the activation regime (between 0 and 0.5 mA cm^{-2}) of ItetS and ItriS.

Sulfonate groups are electron-withdrawing substitutes in aromatic compounds, which can cause an inductive effect on the redox behavior of a species. The sulfonate groups stabilize the reduced form of the indigo dyes by delocalizing electrons throughout the resonance-stabilized molecule. At the same time, this stabilization could inhibit charge transfer at the anode, as the reduced dye would not easily give up electrons. The electronegative, heterocyclic amine group that IC shares with MV would also become more sterically inhibited. This, as well as size and MW, might cause the observed decrease in cell OCV with the addition of sulfonate groups.

4.3. Effect of polar solvents on IC and SAAB performance

In Fig. 2, IC in a 50 mM solution exhibits a constrained polarization under mass transport limitation that yields an $I_{SC} = 4.0$ mA cm^{-2} in a rapid transition from ohmic polarization to short-circuit. In Fig. 3(a), IC in a similar 50 mM solution with 20% vol. DMSO gives a smoother polarization curve descending to $I_{SC} = 5.0$ mA cm^{-2}. The difference in these two cases illustrates the benefit of adding co-solvent, which results in an increase in IC solubility. In Fig. 3(b), the change of I_{SC} as a function of IC concentration indicates that DMSO indeed improves the IC solubility with subsequent effects on dye's electron shuttling capability, including increasing the ionic conductivity (as the ohmic polarization decreased), reducing the influences from mass transport limitation (as the region of ohmic polarization regime extended), and reaching a higher I_{SC} (from 5 to 8 mA cm^{-2}). The presence of 20% vol. DMSO in solution pushed the solubility of IC from less than 50 mM to above 100 mM. The increase of IC ionic conductivity with the IC concentration in solution (as solubility increases) is evident in two aspects: (i) the IR drop of the ohmic polarization region reduced with increasing IC concentration and (ii) the slope of the ohmic polarization region lowered as IC concentration increased.

DMSO might aid charge transfer of the mediator in several ways. A miscible amount of DMSO could reduce viscosity in the solution, not only improving solubility but also fluidity. DMSO could also wet the carbon felt surface better due to reduced viscosity, increasing effective surface area and interaction between the dye and the anode. At the same time, the presence of DMSO lowered cell OCV, likely due to a reduction of solution basicity, which caused the redox dye potential to become more positive.

Several other polar co-solvents were investigated for their ability to improve mass transport of IC in the alkaline solution. Fig. 4 compares the most effective co-solvents, each at 20% vol. in solution and 75 mM IC (chosen arbitrarily to compare the co-solvents at higher IC concentrations). Methanol performed best, achieving an $I_{SC} = 7.2$ mA cm^{-2} even though its performance was constrained by mass transport limitation (seen at 6.5 mA cm^{-2}). In contrast to DMSO, methanol retained solution basicity, producing a cell OCV comparable to that of the nominal solution. The high polarity of methanol and short alkyl group allows greater miscibility with water while still improving dye solubility, fluidity, diffusion, and mass transport. Based on the experience from the study of DMSO, the mass transport limitation should disappear at higher concentrations of IC.

The effect of methanol content on SAAB performance is presented by the study of I_{SC} as a function of methanol % vol., as shown in Fig. 5. There are three notable regions in the range of methanol

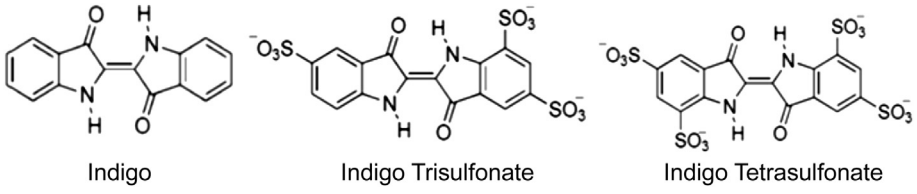

Fig. 7. Molecular structures of indigo, ItriS, and ItetS.

content (0–30% vol.) studied: (1) 0–15% vol., where the I_{SC} increases linearly with methanol content, (2) 15–25% vol., where I_{SC} decreases with methanol content, and (3) ≥25% vol., where I_{SC} seems to reach a stable level. In region (1), similar to DMSO, the presence of co-solvent methanol aids the increase in IC solubility, thus improves the ionic conductivity and I_{SC}. In region (2), the results suggest that the presence of too much polar co-solvent undermined I_{SC}; a phenomenon that requires further study. One hypothesis is that IC has greater affinity toward protons than water and methanol, which increases basicity as suggested by OCV but also impedes IC mobility. Furthermore, excess methanol may cause immiscibility in the solution. At >25% vol. methanol, the solution was separated into two liquid layers. An inevitable consequence of immiscibility is the specific IC solubility in each liquid layer should vary. The aqueous layer should contain more glucose and hydroxide; therefore, the ene-diol intermediate as well; whereas, IC might be preferentially present in the methanol layer. The tendency toward immiscibility and its consequence would explain the result in region (3), since the immiscibility may have created a limiting condition for I_{SC}, making the solubility of IC in one of the liquid layers constrained and attributing to a finite, limiting current in power generation. The complexity of miscibility and solvation may determine the eventual solubility and mobility of mediator in a polar co-solvent electrolyte system, an important consideration in optimizing electrolyte composition.

As the optimal content of methanol co-solvent in the SAAB electrolyte was determined, as shown in Fig. 5, where 15% vol. methanol exhibits the highest I_{SC}, the result of an SAAB with 100 mM IC is exhibited in Fig. 6, juxtaposed with that of a 50 mM IC nominal cell. Indeed, as expected, the improved mass transport in the 15% vol. methanol cell exhibits an extended ohmic polarization region until short-circuit eliminating the nominal limitations of mass transport to achieve an $I_{SC} = 8$ mA cm^{-2}. In contrast, the 50 mM IC cell achieved an $I_{SC} = 4$ mA cm^{-2}.

Disregarding the solubility limit in different solutions, it is always useful to compare results with the same IC concentration. In this case, the IC concentration in the nominal alkaline solution is used as the basis for comparison. Therefore, a scheme was devised in this work to estimate an "equivalent" concentration of the mediator in different solutions. This scheme was informed by the observation that the polarization curve of 100 mM IC with 20% vol. DMSO (Fig. 3(a)) resembles that of 100 mM IC with 15% vol. methanol (Fig. 6), achieving $I_{SC} = 8.0$ mA cm^{-2} in each case. The resemblance in the polarization behavior implies that the effective concentration and mobility of IC, respectively, may be very similar in these two solutions. This might suggest that the mobility is insensitive to changes in IC concentration and solution composition (between different co-solvents), at least in the solubility range studied. In other words, the "equivalent" concentration of IC in both solutions should be similar. With this reasoning, Fig. 3(b) shows two comparative trend lines: the dashed line is the actual correspondence of I_{SC} as a function of IC concentration in 20% vol. DMSO, and the dotted line the corresponding curve in the nominal alkaline solution, with the same slope as that of the 20% vol. DMSO solution. Again, the basis for using the same slope is that IC mobility is insensitive to IC concentration and co-solvent composition. Accordingly, to achieve $I_{SC} = 5$ mA cm^{-2} as in 50 mM IC in 20% vol. DMSO, it would take an "equivalent" 67 mM of IC in the nominal alkaline solution to produce the same. Thus, there is a 33% enhancement in IC solubility with the 20% vol. DMSO co-solvent.

Ultimately, the power density curves in Fig. 6 exhibits a dilemma in optimizing power generation. Although I_{SC} of the improved SAAB nearly doubled with 100 mM IC in 15% vol. methanol solution, its PPD and MPP are roughly the same, within a margin of 100 μW cm^{-2}, as those of the 50 mM IC cell with nominal solution. The distinct differences between the two power density profiles shown in Fig. 6 are observed near the MMP (3.5–4.0 mA cm^{-2}) and beyond (>4.0 mA cm^{-2}). The optimized SAAB exhibited the entire polarization behavior, with the MPP clearly identifiable. The 50 mM IC nominal cell initially produced an identical power density profile until about 2 mA cm^{-2}, beyond which mass transport limitation began to hinder kinetics and power generation. Hence, if the 50 mM IC nominal cell operated beyond the MPP, its polarization quickly reached the short-circuit, indicative of constrained mass transport by the IC concentration limit. Thus, on one hand, the IC solubility was enhanced from 50 mM in nominal solution to 100 mM IC in 15% vol. methanol to increase I_{SC}. On the other, both solutions exhibit a similar MPP and power density profile indicating the enhanced mass transport did not aid the PPD generation. The results suggest that to improve PPD, we need to seek improved charge transfer kinetics to minimize activation loss.

5. Conclusion

In searching for better mediators for applications in the sugar–air alkaline battery (SAAB) to improve power and energy density, 45 redox dyes were studied. Four aspects were considered in the selection of redox dyes: (1) high open circuit voltage; (2) high short-circuit current density (I_{SC}); (3) high solubility; and, (4) low molecular weight. Aside from methyl viologen, indigo carmine and its sulfonate derivatives are attractive for future consideration. To increase dye solubility, protic and aprotic polar co-solvents were added to the nominal alkaline solution. By varying the amount of dye and polar co-solvent in solution, implications of dye solubility and mobility were assessed and analyzed using I_{SC} and peak power density (PPD). The addition of 15% vol. methanol in the nominal alkaline solution with 100 mM IC in the SAAB lowered the polarization resistance, extended the ohmic polarization region, delayed mass transport limitation, and achieved an $I_{SC} = 8$ mA cm^{-2} and a PPD of roughly 800 μW cm^{-2}. Although I_{SC} nearly doubled, the maximum power point (MPP) and PPD of the cell were not improved. The impacts of using polar co-solvents in solution on kinetics were discussed. A study of indigo dye and its sulfonate derivatives provided some insightful information on the effect of molecular structure with various degrees of electronegative substituents have on reaction kinetics and cell performance. Further improvements of energy density and power output need to address the fundamental chemistry to enhance ene-diol production and charge transfer efficiency, as well as mass transport of the mediator in the electrolyte solution.

Acknowledgments

We would like to thank the support provided by the Hawaii Energy & Environmental Technology initiative funded by the Office of Naval Research and the assistance of Dr. Chien-Chen Chiu in the experiments. R. Eustis would like to thank the Department of Chemistry at Whitman College, specifically Allison Calhoun and Marion Gotz for their advice.

References

[1] J.L. Sawin, W.R. Moomaw, Renewable Revolution: Low-carbon Energy by 2030. Worldwatch Report, Worldwatch Institute, Washington, DC, 2009.
[2] A.V. da Rosa, Fundamentals of Renewable Energy Processes, in: Fuel Cells, Academic Press, Waltham, MA, 2013 (Chapter 9).
[3] T.H. Wen, H.Y. Tzu, D.C. Tsang, N.H. Cheng, Appl. Energy 88 (2011) 3990–3998.
[4] R.A. Huggins, J. Power Sources 153 (2006) 365–370.
[5] S.J. Visco, E. Nimon, B. Katz, L.C.D. Jonghe, M.Y. Chu. Abstract 0389, in: The 210th Electrochemical Society Meeting Abstracts, Cancun, Mexico, Vol. 2006-2, 2006.
[6] K.M. Abraham, Z. Jiang, J. Electrochem. Soc. 143 (1996) 1.

[7] T. Ogasawara, A. Débart, M. Holzapfel, P. Novak, P.G. Bruce, J. Am. Chem. Soc. 128 (2006) 1390.
[8] T. Zhang, N. Imanishi, Y. Shimonishi, A. Hirano, Y. Takeda, O. Yamamoto, N. Sammes, Chem. Commun. 46 (2010) 1661–1663.
[9] S.D. Minteer, B.Y. Liaw, M.J. Cooney, Curr. Opin. Biotechnol. 18 (2007) 228–234.
[10] Z. Chen, D. Higgins, A. Yu, L. Zhang, J. Zhang, Energy Environ. Sci. 4 (2011) 3167–3192.
[11] S. Pylypenko, S. Mukherjee, T.S. Olson, P. Atanassov, Electrochim. Acta 53 (2008) 7875–7883.
[12] A.M. Castro Luna, A.E. Bolzkn, M.F. de Mele, A.J. Arvia, Pure Appl. Chem. 63 (1991) 1599–1608.
[13] J.P. Spets, Y. Kiros, T. Noponen, M.A. Kuosa, J. Rantanen, M.J. Lampinen, K. Saari, Open Fuels Energy Sci. J. 2 (2009) 82–86.
[14] T. Chen, S.C. Barton, G. Binyamin, Z.Q. Gao, Y.C. Zhang, H.H. Kim, A. Heller, J. Am. Chem. Soc. 123 (2001) 8630–8631.
[15] N. Mano, F. Mao, A. Heller, J. Am. Chem. Soc. 125 (2003) 6588–6594.
[16] E. Katz, A.N. Shipway, I. Willner, in: W. Vielstich, H.A. Gasteiger, A. Lamm (Eds.), Handbook of Fuel Cells – Fundamentals, Technology and Applications, Fundamentals and Survey of Systems, vol. 1, John Wiley & Sons, Ltd., 2003 (Chapter 21).
[17] S.K. Chaudhuri, D.R. Lovley, Nat. Biotechnol. 21 (2003) 1229–1232.
[18] H. Richter, K. McKarthy, K.P. Nevin, J.P. Johnson, V.M. Rotello, D.R. Lovley, Langmuir 24 (2008) 4376–4379.
[19] T. Ikeda, K. Kano, J. Biosci. Bioeng. 92 (2001) 9–18.
[20] D. Scott, B.Y. Liaw, Energy Environ. Sci. 2 (2009) 965–969.
[21] D. Scott, T.H. Tsang, L. Chetty, S. Aloi, B.Y. Liaw, J. Power Sources 196 (2011) 10556–10562.
[22] D.R. Wheeler, J. Nichols, D. Hanson, M. Andrus, S. Choi, D. Watt, J. Electrochem. Soc. 156 (2009) B1201–B1207.
[23] S. Kerzenmacher, J. Ducrée, R. Zengerle, F. Stetten, J. Power Sources 182 (2008) 1–17.
[24] S. Park, H. Boo, T.D. Chung, Anal. Chim. Acta 556 (2006) 46–57.
[25] Z. Wei, W. Huang, S. Zhang, J. Tan, J. Power Sources 91 (2000) 83–85.
[26] J. Hill, E. Nelson, D. Tilman, S. Polasky, D. Tiffany, Proc. Natl. Acad. Sci. U. S. A. 103 (2006) 11206–11210.
[27] E.S. Guzman Barron, L.A. Hoffman, J. Gen. Physiol. 13 (1930) 483–494.
[28] K.P.C. Vollhardt, N.E. Schore, Organic Chemistry: Structure and Function, W.H. Freeman and Company, New York, 2007, pp. 1146–1154.
[29] M. Ishiyama, M. Shiga, K. Sasamoto, M. Mizoguchi, P. He, Chem. Pharm. Bull. 41 (1993) 1118–1122.
[30] R. Bourbonnais, D. Leech, M.G. Paice, Biochim. Biophys. Acta Gen. Subj.1379 (1998) 381–390.
[31] A. Turcanu, T. Bechto, Dyes Pigm. 91 (2011) 324–331.
[32] M.C. Costa, F.S.B. Mota, A.B.D. SantosI, G.L.F. Mendonça, R.F. Nascimento, Quím Nova 35 (2012). São Paulo, S0100-40422012000300008.
[33] H.W. Jacob, Methods Microbiol. 2 (1970) 97–123.
[34] P. Wardman, J. Phys, Chem. 18 (1989) 1637–1755.
[35] F. Van der Zee, Doctoral thesis, Anaerobic Azo Dye Reduction, Wageningen University, Wageningen, The Netherlands, 2002, 90-5808-610-0.
[36] P. Tratnyek, T. Reilkoff, A. Lemon, M. Scherer, B. Balko, L. Feik, B. Henegar, Chem. Educ. 6 (2001) s00897010471a.
[37] P.M. Gallop, M.J. Glimcher, M.A. Paz, R.A.B. Ezekowitz, J. Neurosci. 12 (1992) 2362–2369.
[38] Sigma-Aldrich Co. LLC, (2012), PN33150
[39] N. Menek, Turk. J. Chem. 27 (2003) 155–166.
[40] S.A. Wilson, J.H. Weber, Chem. Geol. 26 (1979) 345–354.
[41] A. Hulanicki, S. Glab, Pure Appl. Chem. 50 (1978) 463–498.